General Disclaimer

One or more of the Following Statements may affect this Document

- This document has been reproduced from the best copy furnished by the organizational source. It is being released in the interest of making available as much information as possible.

- This document may contain data, which exceeds the sheet parameters. It was furnished in this condition by the organizational source and is the best copy available.

- This document may contain tone-on-tone or color graphs, charts and/or pictures, which have been reproduced in black and white.

- This document is paginated as submitted by the original source.

- Portions of this document are not fully legible due to the historical nature of some of the material. However, it is the best reproduction available from the original submission.

A THRUST-SHEET PROPULSION CONCEPT USING FISSIONABLE ELEMENTS

by W. E. Moeckel
Lewis Research Center
Cleveland, Ohio 44135

A THRUST-SHEET PROPULSION CONCEPT USING FISSIONABLE ELEMENTS

by W. E. Moeckel
National Aeronautics and Space Administration
Lewis Research Center
Cleveland, Ohio 44135

Abstract

A space propulsion concept is proposed and ana-
lyzed which consists of a thin sheet coated on one
side with fissionable material, so that nuclear
power is converted directly into propulsive power.
Thrust is available both from ejected fission frag-
ments and from thermal radiation. Optimum thick-
nesses are determined for the active and substrate
layers. This concept is shown to have potential
mission capability (in terms of velocity increments)
superior to that of all other advanced propulsion
concepts for which performance estimates are avail-
able. A suitable spontaneously fissioning material
such as Cf^{254} could provide an extremely high-
performance first stage beyond Earth orbit. In
contrast with some other advanced nuclear propul-
sion concepts, there is no minimum size below which
this concept is infeasible.

More mission versatility would result if the
thrust-sheet fission rate were controllable with an
auxiliary system that produces fission-triggering
neutrons or photons. Known neutron sources, how-
ever, are found to be much too heavy. Similarly, a
system to produce photons with energy sufficient
for photo fission is likely to be too heavy. Thus,
the concept of a controlled-fission thrust sheet is
currently purely hypothetical.

Introduction

Deep space mission capabilities of the most
advanced propulsion concepts for which performance
estimates are available were discussed and compared
in Refs. 1 and 2. (Sources for the performance
estimates are listed in those references.) The
comparison showed that pulsed-fusion or gaseous-
core fission rockets could produce the fastest trip
times to the near planets, while magnetically
contained fusion could provide the best capability
for more distant destinations. These conclusions
assumed that the estimated performances of these
conceptual systems were ultimately achievable in
practice. With these performances, round trips to
Mars could be accomplished in a few months and
round trips to the outer planets in several years.
Although these trip times represent order-of-
magnitude improvements over chemical rockets, one
wonders whether even better propulsion systems can
be conceived, and what form they might take.

A common assumption is that the ultimate pro-
pulsion system would be a photon rocket, where the
photons are produced by mass annihilation (matter-
antimatter reactions).[3,4] Such a system would
produce the highest possible exhaust velocity, and
the ultimate in conversion of propellant mass into
propulsive energy. However, no conceptual basis is
available to evaluate such a system, since no vi-
able ways have been proposed to produce, store, and
recombine antimatter without introducing auxiliary
system masses in excess of those needed for previ-
ously proposed fission and fusion propulsion con-
cepts. The limitations on these fission and fusion
concepts as pointed out in Ref. 1, are due neither

to a low fraction of conversion of matter into
energy, nor to the unattainability of high exhaust
velocity. Instead, the performance limits result
from the problems of thermal power containment and
the conversion of that thermal power into directed
propulsion power. These conversion problems would
be accentuated for the photon rocket due to the
very energetic photons produced by mass annihila-
tion reactions. The resulting inert mass needed
for containment, cooling, shielding, and conversion
to thrust could easily exceed that of fission or
fusion reactors, thereby nullifying the possible
benefits of increased exhaust velocity and mass-
energy conversion fraction.

Thus, the progression from fission or fusion
to mass annihilation reactions may not of itself
yield improved propulsion performance. It is
therefore desirable to consider alternative ap-
proaches. Particularly desirable would be elimina-
tion of the need for a hot high-density power
source, with its associated inert mass requirements.

This paper describes and analyzes an alterna-
tive approach whereby the necessary high exhaust
velocities can be achieved with good thrust/mass
ratio. This approach involves the concept of a
large-area thin sheet which produces thrust by
spontaneous or stimulated ejection of fission frag-
ments from its rearward surface. It involves use
of nuclear fission characteristics which may be
found among the transuranic elements. The charac-
teristics of such thrust sheets are analyzed and
optimum thicknesses for the component layers are
evaluated (Appendix A). Included in the analysis
of this concept is the possibility of deriving sig-
nificant thrust from differential thermal radiation,
obtainable by producing different emissivities on
the forward and rearward surfaces.

Discussion of Previous Propulsion Concepts

Shown in Fig. 1 (slightly modified from
Ref. 2)[*] are the primary performance parameters
estimated to be attainable with previously analyzed
advanced propulsion concepts. For the systems
labeled type I (relatively high thrust/mass ratio)
the mission capability is determined primarily by
the exhaust velocity attainable; while for systems
labeled type II (low thrust/mass ratio) the mission
performance is determined primarily by the specific
power attainable. This figure shows that to pro-
duce mission capability superior to those previ-
ously analyzed, one needs systems with specific
power above about 1 kilowatt of jet power per kilo-
gram of propulsion system mass, and exhaust veloc-
ity above about 50 km/sec (specific impulse above
5000 sec). To achieve the 50 km/sec exhaust ve-
locity level with the type I systems shown in
Fig. 1 required either a very high-temperature gas
source (gas-core nuclear fission rocket) or a

---

[*]Specific power (propulsive power/mass of propul-
sion system) is used as the abscissa, instead of
its reciprocal (specific mass) to conform more
closely with current practice.

series of small thermonuclear explosions (pulsed-fusion rocket). To achieve a specific power of about 1 kilowatt per kilogram with a type II system also requires an extremely high temperature power source (controlled thermonuclear fusion reactor). Each of these concepts involves considerable optimism with regard to future technological achievements; they seem close to the limits of performance attainable with high power density thermal sources.

A few propulsion concepts have been proposed and analyzed over the years which do not involve high density on-board thermal sources. These include solar sails,[5,6] laser-propelled sails,[7] and radioisotope sails.[8] This general class of propulsion concepts characterized by impingement on, or emission from, large area thin sheets will be called "thrust-sheet propulsion."

The impinging-photon thrust sheets showed performance comparable to other advanced systems, but were more limited in that they could operate only within the range of their photon source. Solar sails are comparable in mission performance capability to solar-electric propulsion, but lack the versatility. Laser-propelled sails require tremendous ratios of power to thrust, and are not competitive with other advanced concepts even for one-way flyby missions unless extremely powerful highly comminated x-ray lasers can be developed.

The radioisotope thrust sheet[8] has received little attention or analysis, primarily because it seemed to offer little advantage in mission capability over solar sails, and appeared to have more difficult development problems (heat dissipation and energy decay during storage, expense, and handling difficulties of the radiative coating, etc.). The radioisotope considered most suitable in Ref. 8 (Polonium 210) has a half-life of 138 days and a very respectable initial energy release rate (specific power) of 141 kW/kg, consisting of 5.3 MeV α-particles. The maximum possible exhaust velocity (ejection velocity) is about 1.5×10^7 m/sec. A cursory calculation yields a possible thrust per unit area of the thrust sheet of about 5×10^{-4} N/m^2, and a thrust-mass ratio of 2×10^{-3} m/sec^2, which is comparable with values obtainable with solar sails at Earth orbit.

Although the Po^{210}-coated thrust sheet has attracted little attention, it has many of the desirable features of an ideal propulsion system. It produces thrust directly at very high exhaust velocity in the simplest possible manner, with no auxiliary mass for containment, redirection, shielding, or cooling. It is self-contained (does not depend on an external radiation source), and is insensitive to environmental hazards such as radiation and micrometeoroid damage. Thus, if such a system could produce velocity increments (Δv) much greater than competitive concepts, the development and operational problems might be worth the effort to solve.

The primary reason that the Po^{210} thrust sheet cannot achieve large superiority in Δv is that the ratio of inert mass to ejected (propellant) mass is large - at best equal to the ratio of Po^{210} to α-particle mass, or about 50. The magnitude of this handicap can be seen from the rocket equation:

$$\Delta v = v_j \ln \frac{m_o}{m_1} = v_j \ln \left(1 - \frac{m_p}{m_o} \right)^{-1} \qquad (1)$$

where v_j is effective exhaust velocity, m_o is total initial mass and m_1 is the residual mass (after exhausting the propellant mass, m_p). Equation (1) shows that for $m_p/m_o = 1/50$, the Δv achievable is only about $v_j/50$. Hence, for Po^{210}, with maximum v_j of 1.5×10^7 m/sec, the maximum Δv is about 3×10^5 m/sec.

A more detailed analysis of the performance of particle-emitting thrust sheets is given in Appendix A, wherein the losses in momentum and energy of emitted particles due to isotropic emission and collisions within the imbedding material are considered. This analysis shows that, even for optimum active-film and substrate thicknesses, the achievable Δv may be less than 10^{-3} of the particle ejection velocity (Eq. (A49)), or about 10^4 m/sec, which is less than 10 percent of the value estimated above. The effective v_j (from Eq. (A49)) is about 3.3×10^6 m/sec, and the vehicle thrust/mass ratio (Eq. (A50)) is about 7×10^{-4} m/sec^2. These values are shown in Fig. 1 for comparison with other propulsion concepts. The performance capability is inferior to that, for example, of a gaseous-core nuclear fission rocket concept, for which v_j may be lower ($<5 \times 10^4$ m/sec) but m_p/m_o may be of order 0.8 yielding a Δv of about 8×10^4 m/sec.

One is thus led to contemplate ways in which the admirable features of the Po^{210} thrust sheet can be retained, while the effective ratio of propellant to inert mass is substantially increased. If it were possible to eject somehow the spent residue (Pb^{206}) of the Po^{210} decay, so that it would not accumulate as inert mass, then the "propellant" ratio would increase to about 0.5 (the substrate sheet would still remain) but the effective exhaust velocity would be reduced by a factor of 50, since the Pb^{206} residue would essentially be ejected with zero velocity. Equation (1) shows that this tradeoff increases $\Delta v/v_j$ to 0.7, but this is insufficient to compensate for the reduction in the effective v_j; hence Δv is not improved.

Spontaneous-Fission Thrust Sheets

A clear possibility for improvement lies in the use of a decay process that ejects a much larger fraction of the parent nucleus. A spontaneous fission process with approximately equal-mass remnant nuclei would yield the maximum possible ejected-mass fraction for a spontaneous-emission thrust-sheet propulsion system. Examination of charts of the nuclides[9] reveals a number of nuclei among the transuranium elements that undergo spontaneous fission. For many of these nuclei, however, the fission process is subordinate to other decay processes. For others the half-life is much too small to be suitable for propulsion or much too long to produce significant specific power. One interesting candidate nucleus seems to be Californium 254 which undergoes fission with half-life of 60 days (or 65 days, according to Ref. 10). If the mean fission energy release is of the order of 200 MeV, (it is given as 185 MeV in Ref. 10), the fission fragment velocity will be about 1.2×10^7 m/sec.

2

With the reduction due to isotropic emission and collisional losses in the film and for optimized substrate and active-film thickness (as calculated in Appendix A), the effective exhaust velocity (Eq. (A48)) becomes 1.9×10^6 m/sec, and the initial thrust/mass ratio (Eq. (A44)) is about 0.025 m/sec^2. Addition of the thrust possible with differential thermal radiation (Eq. (A46)) yields net thrust/mass ratio of about 0.033 (Eq. (A50)). These values are indicated in Fig. 1 for comparison with other concepts. The Δv is about 2.2×10^5 (Eq. (A48)) which is more than twice that achievable with the best previously analyzed type I systems of Fig. 1 ($\approx 8 \times 10^4$ m/sec for $v_j = 5 \times 10^4$, $m_p/m_o = 0.8$).

To evaluate the significance of this increased Δv in terms of mission capability, consider the distances attainable as functions of time in field-free space. (Ref. 2 showed that for higher-performance propulsion systems, field-free estimates are good approximation for almost all missions except those that descend into or depart from low orbits about the major planets). The acceleration of a vehicle propelled by a spontaneously emitting thrust sheet is:

$$a = a_o e^{-0.693\, t/\tau} \qquad (2)$$

Integration of Eq. (2) yields:

$$v = 1.44\, a_o \tau (1 - e^{-0.693\, t/\tau}) \qquad (3)$$

and the distance traveled is

$$X = 1.44\, a_o \tau^2 \left[\frac{t}{\tau} - 1.44(1 - e^{-0.693\, t/\tau}) \right] \qquad (4)$$

If X is expressed in astronomical units (1 Au = 1.495×10^{11} m) and t in days, this becomes

For Cf^{254}:

$$X = 8.5 \left[\frac{t}{60} - 1.44(1 - e^{-0.693\, t/60}) \right] \qquad (5)$$

and for Po^{210}:

$$X = 0.84 \left[\frac{t}{138} - 1.44(1 - e^{-0.693\, t/138}) \right] \qquad (6)$$

where the values of a_o were obtained from Eq. (A50).

Equations (5) and (6) are plotted in Fig. 2 for one-way fly-by missions to the outer solar system. Shown also are curves for the best type I and type II propulsion concepts of Ref. 2 and for a solar sail (Appendix B). The figure shows that the Cf^{254} thrust sheet concept has capabilities superior to those attainable with the most optimistic propulsion system parameters estimated for the other advanced concepts. Such a thrust sheet could serve as the entire propulsion system (beyond Earth orbit) for fly-by missions or for missions lasting no longer than a few half-lives of the active material. It could also serve as a high-performance first-stage (beyond Earth orbit) for longer rendezvous or round-trip missions.

Controlled-Fission Thrust Sheets

Even more desirable than a spontaneously fissioning material such as Cf^{254} would be a material whose fission could be induced at will by means of some lightweight auxiliary system. Such a sheet would eliminate the limitation of spontaneous-emission thrust sheets to one-way missions or to the first stage of more lengthy missions. The total impulse available with a controlled-fission thrust sheet would be comparable to that of a spontaneous-fission thrust sheet, but the impulse could be divided and allocated according to mission needs.

One might consider first the possibility of using a common fission reactor material in the active film (say uranium or plutonium) so that it could be activated with a source of thermal or fast neutrons. Calculations show, however, that the obvious neutron sources, such as fission or fusion reactors, would be much too heavy to serve as the auxiliary system. In fact, it is more effective in propulsion capability to use the thermal power of such reactors for the other nuclear propulsion systems of Fig. 1 than to use them as neutron sources for thrust-sheet propulsion.

Another possibility is to use a copious spontaneous neutron emitter such as Californium 252, which produces of the order of 10^{15} neutrons/sec-Kg, and has an adequate half-life of 2.64 years. This neutron production rate, however, is found to be inadequate, because the thrust-sheet fission rate needed to produce interesting thrust levels is of the order 10^{15}/sec-m^2; hence one would need at least 1 kilogram of Cf^{252} per meter^2 of thrust sheet, which is a factor of at least 100 too high, even if all neutrons were to produce fission.

Since known neutron sources seem inadequate, one may next consider whether a photon source might be feasible. Photofission has been observed and studied quite extensively[11-13] with thorium, uranium, and neptunium using high-energy photons (MeV range). If nuclei could be found or produced which fission when triggered by lower-energy photons, perhaps an auxiliary system might be devised with sufficiently low mass to provide the desired thrust sheet control.

To estimate the power and mass needed for the auxiliary source for a photofissionable thrust sheet, one must evaluate the fission rate desired to produce adequate acceleration. Using the optimized layer thicknesses derived for Cf^{254} in Appendix A, the active-layer mass density is 0.0375 kg/m^2 (Eq. (A44)) and the fission rate is $\approx 10^{16}$ fissions/m^2-sec. If a fraction f of impinging photons produced fissions, then the photon power per m^2 becomes

$$P = \frac{10^{16}}{f} (h\nu)\, W/m^2 \qquad (7)$$

and the auxiliary power (presumably nuclear-electric) needed to produce this photon flux is

$$P_e = P/\eta \qquad (8)$$

where η is the overall efficiency of converting electric power into photon power. If α' is the specific power of the electric generator system

(We/kg), then the ratio of auxiliary-power mass m_a to thrust-sheet mass m_s is

$$\frac{m_a}{m_s} = \frac{P_e}{m_s \alpha'} = \frac{10^{16} h\nu}{\eta f m_s \alpha'} \qquad (9)$$

With $m_s \simeq 0.07$ kg/m^2 (see Eq. (A48)), $\alpha' = 10^2$ W/kg, and $h\nu = hc/\lambda = 2 \times 10^{-25}/\lambda$, we have

$$m_a/m_s = \frac{3 \times 10^{-10}}{\eta f \lambda} \qquad (10)$$

Clearly, unless $\lambda \geq 10^{-9}$ m $= 10$ Å, auxiliary equipment is likely to outweigh the thrust sheet. For $\lambda = 300$ nm, however, the product ηf can be as little as 10^{-3} without seriously affecting the inert mass of the system. Thus, if nuclei could be found or made that are fissionable with near-optical range photons and with high fission cross section, one might achieve the superior performance capability of a controllable thrust-sheet propulsion system.

The probability that nuclides can be produced which are fissionable with such low-energy photons, however, seems vanishingly small since such photons interact only with the outer electron shells of the atom. The likelihood that such a small perturbation could significantly affect a nuclear process seems negligible. Thus, the concept of a fission-powered thrust sheet propulsion system with controllable fission rate must be regarded as hypothetical.

Concluding Remarks

The fission-powered thrust sheet concept proposed and analyzed herein has, of course, many practical difficulties not yet discussed. These include (1) construction, deployment, and controllability, (2) payload shielding from fission-produced neutrons and γ-radiation, (3) producibility and cost of the fissionable material, and (4) maintenance of sheet integrity under the severe radiation conditions.

The first group of problems is similar to those studied in connection with solar sails[5,6] except that for a spontaneous-fissioning thrust sheet the active material would perhaps have to be applied in space after sheet deployment to avoid the need for a cooling system during launching.

The problem of shielding the payload from undesirable radiation is also not unique to the fission-powered thrust sheet, although with other nuclear propulsion concepts the required shielding is generally considered to be achieved primarily with mass distribution around the reactor. For the thrust sheet, an optimum combination of payload distance, relative location, and shielding mass would be employed.

Perhaps the most critical factor for practical application is the future availability, producibility and cost of suitable transuranium materials. Many transuranium elements are now made by neutron bombardment in nuclear reactors, and some are available in weighable quantity. Major suppliers in the United States are the High-Flux Isotope Reactor Transuranium Processing Facility (HFIR-TRU)

at the Oak Ridge National Laboratory and the Savannah River Plant Transuranium Processing Facility (SRP-TRU). Information in Refs. 14 and 15 indicate that Californium 252 is available at a price of about $10 per microgram, with a possible reduction to about $1 per microgram by the 1980's.[14] Production rate is currently in the range of several grams per year, with increases to hundreds of grams per year estimated for the 1980's. However, Cf^{254} is not available in separated form. It occurs with Cf^{252} at a ratio of about 5×10^{-4}. Enhancement by a factor of 10 or 20 (to perhaps 1 percent of the Cf^{252}) could perhaps be attained in fast breeder power reactors when they become operational.[16] Separation of Cf^{254} from Cf^{252} could presumably be achieved by methods similar to those used to enrich U^{235}.

Another possible source of suitable fissionable materials may be in the so-called "magic island" of stable nuclides in the vicinity of atomic number 114 and atomic mass 300.[17,18] Research is underway to synthesize nuclei in this region. Perhaps some other nuclides with suitable half-lives (or even some easily triggered photofissionable nuclei) will be found in this region.

Because all nuclei with $Z^2/A > 18$ are theoretically unstable against spontaneous fission, the term "stable" is a relative one in the context of transuranium nuclei, and indicates the magnitude of the decay half-life. Consequently, the concept of a threshold energy for stimulating fission is generally not well defined.[19] By neutron or photon bombardment, one tends to enhance the instability and thereby produce a more copious fission rate. The magnitude of the stimulus needed for this cannot be accurately predicted for all nuclei. Nevertheless, as mentioned in the text, the probability of greatly enhancing a nuclear fission rate by means of optical-range photons seems negligible. The nucleus would have to be very unstable (and hence have a very small half-life) in order that such a small perturbation could appreciably affect its decay rate.

Another unknown factor in determining the feasibility of fission-power thrust sheets is the question of maintaining the integrity of the sheet during the propulsion period. As indicated in Appendix A, a retention film will be needed over the active film to retain atoms that would otherwise be knocked out by the emerging fission fragments. Since the optimum substrate thickness permits emergence of some fission fragments in the forward, as well as rearward, direction, a retention film may also be needed on the substrate side. Such a film could also reduce vaporization rate, which must be less than 10^{-7} meter during the propulsion period. If the thickness of these films becomes comparable to the thickness of the active film, serious deterioration of performance results. Indications are, however,[20] that retention film thicknesses of a few hundred Å ($\approx 10^{-8}$ m) may be adequate, in which case the effect on performance is small.

Another question is whether the substrate film will be so severely radiation damaged by the emerging fission fragments that it will not provide the required strength during the propulsion period. As shown in Appendix A (Eq. (A53)), the stress on the substrate is very mild (about 2.5×10^4 N/m^2, (4 psi)) for a 100-meter radius sheet) but the ability to maintain integrity must still be established.

4

Thus, to evaluate whether the attractive mission capabilities of fission-powered thrust sheets can become achievable, several fundamental questions must be answered: (1) Can sufficiently large quantities of Cf^{254} (or perhaps other isotopes with comparable fission half-life) be produced at acceptable cost? and (2) Can the problems of fabrication, deployment, and operation be solved? (3) How thick must retention films be? (4) Can the substrate maintain adequate strength during the thrust period? In addition, some research may be warranted on possible new methods to stimulate fission with low mass auxiliary systems so that the significant advantages of a controlled-fission thrust sheet can be realized.

Appendix A

Analysis of Spontaneous Emission Thrust-Sheet Propulsion

The mass, momentum, and energy that emerges from a sheet containing a spontaneously emitting material must be evaluated to determine the effective propellant ratio, m_p/m_o, effective exhaust velocity, v_j, thrust/mass ratio, and heating of the thrust sheet. This evaluation will be made for the three-layer thrust sheet shown in sketch (a). In this sketch, x_e is the distance of the source of an emitted particle from the rearward surface of the sheet, θ is the emission angle, v_e the velocity of the emitted particle when it emerges from the sheet, and v_{ex} is the thrust component of that velocity. A retention film of thickness d_1 is provided to contain the material of the active film (other than the emitted particles), and a substrate of thickness d_3 is provided to stop forward-moving emitted particles and for support of

x = 0 x_1 x_2 x_3
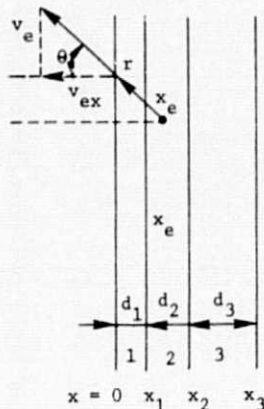
1: Retention layer
2: Active layer
3: Substrate layer

Sketch a: Thrust-sheet nomenclature.

the active film thickness d_2.

Because the emission is isotropic, the fraction of particles emitted at x_e which emerge from the thrust sheet with angles between θ and $\theta + d\theta$ is proportional to the area of the thrust sheet through which they pass, i.e.,

$$\frac{dn}{n} = \frac{dA}{A} = \frac{2\pi r \sin\theta \cdot r \, d\theta}{4\pi r^2} = \frac{1}{2}\sin\theta \, d\theta \qquad (A1)$$

Hence, the fraction of the total emitted particles originating at x_e that emerge from the sheet is

$$\left(\frac{n_e}{n}\right)_{x_e} = \frac{1}{2}\int_0^{\theta_m} \sin\theta \, d\theta = \frac{1}{2}(1 - \cos\theta_m) \qquad (A2)$$

where θ_m is the maximum angle for which particles from x_e can reach the rearward surface:

$$\cos\theta_m = \frac{x_e}{r_m} \qquad (A3)$$

where r_m is the range of the emitted particle in the embedding material. (The velocity-distance variations are assumed to be the same in all three films for simplicity of analysis.) The fraction of all emitted particles (n_o) in the active film that emerge rearward is obtained by integrating Eq. (A2) over the active film:

$$\frac{n_e}{n_o} = \frac{1}{d_2}\int_{x_1}^{x_2}\left(\frac{n_e}{n}\right)_{x_e} dx_e = \frac{1}{2}\left[1 - \frac{1}{2}\frac{d_2 + 2d_1}{r_m}\right] \qquad (A4)$$

With this equation, the vehicle propellant mass ratio can be written,

$$\frac{m_p}{m_o} = \frac{Mn_o(n_e/n_o)}{m_1 + m_2 + m_3 + m_r} \qquad (A5)$$

where M is the emitted-particle mass, the m_i are mass per unit area of the sheet layers, and m_r is all vehicle mass other than thrust sheet (including payload, shielding, attachments, controls, etc.). If μ is the ratio of m_r to thrust-sheet mass, and γ the ratio of emitted-particle mass to emitting-particle mass (M/M_o), Eq. (A5) becomes (since $m_2 = M_o n_o$):

$$\frac{m_p}{m_o} = \frac{\gamma\left[\frac{1}{2} - \frac{1}{4}\frac{d_2}{r_m}\left(1 + 2\frac{d_1}{d_2}\right)\right]}{(1 + \mu)\left(1 + \frac{d_1 + d_3}{d_2}\right)} \qquad (A6)$$

The fraction of the emitted-particle energy that emerges rearward is obtained by a similar double integration:

$$\frac{v_e^2}{v_m^2} = \frac{1}{2d_2}\int_{x_1}^{x_2} dx_e \int_0^{\theta_m}\left(\frac{v_e}{v_m}\right)^2 \sin\theta \, d\theta \qquad (A7)$$

where v_m is the initial ejection velocity of the emitted particles.

Similarly, the mean x-component of the velocity of the emerging particles (which is the effective exhaust velocity v_j) is given by

5

$$\frac{v_j}{v_m} = \frac{\langle v_{ex} \rangle}{v_m} = \frac{1}{2d_2} \int_{x_1}^{x_2} dx_e \int_0^{\theta_m} \left(\frac{v_e}{v_m}\right) \cos\theta \sin\theta \, d\theta \tag{A8}$$

To evaluate Eq. (A7) and (A8), the variation of particle velocity with distance in the embedding material is needed. For fission products, Ref. 21 (p. 669) indicates that, if one neglects a "plateau" region near the end of their range, the required variation is well represented by

$$\frac{v}{v_m} = 1 - \frac{r}{r_m} \tag{A9}$$

where $r_m \approx 2$ cm in air for intermediate-mass fission fragments, and $v_m \approx 1.2 \times 10^7$ m/sec. For embedding materials other than air, the range is well approximated by the Bragg-Kleemann rule

$$\frac{\rho r_m}{(\rho r_m)_{air}} = \sqrt{\frac{A}{A_{air}}} \tag{A10}$$

where A is atomic mass units of the embedding material, $\rho_{air} = 1.2$ kg/m^3, and $A_{air} = 14.5$. A table in Ref. 21 (p. 671) shows that Eq. (A10) works well for α-particles as well as fission fragments.

The velocity-distance relation for α-particles, however, is not well represented by Eq. (A9). A better representation of the data shown in Ref. 21 (p. 649) is

$$\frac{v}{v_m} = \left(1 - \frac{r}{r_m}\right)^{1/2} \tag{A11}$$

where $r_m \approx 4$ cm in air, and v_m for Po^{210} α-particles is about 1.6×10^7 m/sec.

With Eq. (A9) and (A11), Eq. (A7) and (A8) become:

$$\frac{\langle v_e^2 \rangle}{v_m^2} = \frac{1}{2d_2} \int_{x_1}^{x_2} dx_e \int_0^{\theta_m} \left(1 - \frac{x_e/r_m}{\cos\theta}\right)^{2a} \sin\theta \, d\theta \tag{A12}$$

$$\frac{v_j}{v_m} = \frac{1}{2d_2} \int_{x_1}^{x_2} dx_e \int_0^{\theta_m} \left(1 - \frac{x_e/r_m}{\cos\theta}\right)^a$$

$$\times \cos\theta \sin\theta \, d\theta \tag{A13}$$

where $a = 1$ for fission fragments and $a = 0.5$ for α-particles.

With the substitutions $\xi = x_e/r_m$ and $y = \xi/\cos\theta$ these equations become:

$$\frac{\langle v_e^2 \rangle}{v_m^2} = \frac{r_m}{2d_2} \int_{\xi_1}^{\xi_2} \xi \, d\xi \int_1^{\xi} - (1 - y)^{2a} y^{-2} \, dy \tag{A14}$$

$$\frac{v_j}{v_m} = \frac{r_m}{2d_2} \int_{\xi_1}^{\xi_2} \xi \, d\xi \int_1^{\xi} - (1 - y)^a y^{-3} \, dy \tag{A15}$$

For $a = 1$ (fission-fragment case):

$$\frac{\langle v_e^2 \rangle}{v_m^2} = \frac{1}{2}\left[1 - \frac{1}{2}\frac{d_2}{r_m}\left(1 + 2\frac{d_1}{d_2}\right) - \frac{1}{3}\left(\frac{d_2}{r_m}\right)^2\left(1 + 3\frac{d_1}{d_2} + 3\frac{d_1^2}{d_2^2}\right)\right.$$

$$\left. + \frac{d_2}{r_m}\left(1 + \frac{d_1}{d_2}\right)^2 \ln\frac{d_2}{r_m}\left(1 + \frac{d_1}{d_2}\right) - \frac{d_2}{r_m}\left(\frac{d_1}{d_2}\right)^2 \ln\frac{d_1}{r_m}\right] \tag{A16}$$

$$\frac{v_j}{v_m} = \frac{1}{4} - \frac{1}{4}\frac{d_2}{r_m}\left(1 + 2\frac{d_1}{d_2}\right) + \frac{1}{12}\left(\frac{d_2}{r_m}\right)^2\left(1 + 3\frac{d_1}{d_2} + 3\frac{d_1^2}{d_2^2}\right) \tag{A17}$$

For $a = 1/2$ (α-particle case):

$$\frac{\langle v_e^2 \rangle}{v_m^2} = \frac{1}{2} - \frac{3}{8}\frac{d_2}{r_m}\left(1 + 2\frac{d_1}{d_2}\right) + \frac{1}{4}\frac{d_2}{r_m}\left(1 + \frac{d_1}{d_2}\right)^2$$

$$\times \ln\frac{d_2}{r_m}\left(1 + 2\frac{d_1}{d_2}\right) - \frac{1}{4}\frac{d_2}{r_m}\frac{d_1^2}{d_2^2}\ln\frac{d_1}{r_m} \tag{A18}$$

No closed-form integral of Eq. (A15) was found with $a = 1/2$; hence an approximate solution was obtained by substituting $y = \eta^{-1}$, and using an approximation for the resulting integrand:

$$\sqrt{\eta(\eta - 1)} \approx \eta - 0.5$$

With this approximation, Eq. (A15) becomes ($a = 1/2$):

$$\frac{v_j}{v_m} = \frac{1}{4} - \frac{1}{8}\frac{d_2}{r_m}\left(1 + 2\frac{d_1}{d_2}\right) \tag{A19}$$

With Eq. (A6), (A17), and (A19) expressions for Δv for thrust sheets using spontaneous fission or α-particle decay can be obtained.

The thrust-mass ratio (acceleration) of the thrust sheet-propelled vehicle, which determines its field-free trajectory (Eq. (4)), is obtained from

$$\frac{F}{m_0} = a = \frac{\dot{m}_p v_j}{m_0} = \frac{0.693}{\tau}\left(\frac{m_p}{m_0}\right)\left(\frac{v_j}{v_m}\right)v_m e^{-0.693 \, t/\tau} \tag{A20}$$

where τ is the half-life of the emitting material, m_p/m_0 is given by Eq. (A6) and v_j/v_m is calculated from Eq. (A17) or (A19). Separating out the factors that are functions only of the thickness ratios Eq. (A20) can be written:

$$a = \frac{0.693 \, v_m \gamma}{\tau(1 + \mu)} f\left(\frac{d_2}{r_m}, \frac{d_1}{d_2}\right) e^{-0.693 \, t/\tau} \tag{A21}$$

where

$$f\left(\frac{d_2}{r_m}, \frac{d_1}{d_2}\right) = \frac{\left[\frac{1}{2} - \frac{1}{4}\frac{d_2}{r_m}\left(1 + 2\frac{d_1}{d_2}\right)\right]\left[\frac{1}{4} - \frac{a}{4}\frac{d_2}{r_m}\left(1 + 2\frac{d_1}{d_2}\right)\right]}{1 + \frac{d_1 + d_3}{d_2}} \qquad (A22)$$

The $(d_2/r_m)^2$ factor in Eq. (A17) is generally negligible and has been omitted in (A22). Inserting the appropriate values of v_m, γ, and τ in Eq. (A21) yields, for the initial accelerations:

For Cf^{254} ($v_m = 1.2 \times 10^7$, $\gamma = 0.5$, $\tau = 60$ days):

$$a_o = \frac{0.8}{1 + \mu} f\left(\frac{d_2}{r_m}, \frac{d_1}{d_2}\right) m/sec^2 \qquad (A23)$$

and for Po^{210} ($v_m = 1.6 \times 10^7$, $\gamma = 0.02$, $\tau = 138$ days):

$$a_o = \frac{0.018}{1 + \mu} f\left(\frac{d_2}{r_m}, \frac{d_1}{d_2}\right) m/sec^2 \qquad (A24)$$

Acceleration Due to Differential Thermal Radiation

In addition to the particle-emission thrust, an acceleration can also be obtained if the thermal emissivity of the forward surface of the thrust sheet is lower than that of the rearward surface. (The temperature of the two surfaces is assumed to be the same, since it would be difficult to achieve a significant temperature difference in such thin sheets.) To evaluate the magnitude of this additional thrust, note that the radiation pressure is equal to radiation power density divided by the velocity of light, c. Hence, the net acceleration due to differential radiation is

$$a_r = \frac{\Delta p}{m_o} = \frac{\sigma(\varepsilon_r - \varepsilon_f)T^4}{cm_o} \qquad (A25)$$

where ε_r and ε_f are the thermal emissivities of the rearward and forward surfaces, respectively.

The temperature T of the thrust sheet is determined by the equilibrium between generated power and radiated power per unit area. The former is given by

$$P_g = \dot{n}E = \frac{m_2 E}{M_o}\left(\frac{0.693}{\tau}\right)e^{-0.693\ t/\tau} \qquad (A26)$$

where E is the energy release per particle in the active layer and M_o (= 1.66×10^{-27} A_2) is the emitting-particle mass. Setting this power equal to the radiated power yields:

$$\sigma T^4 = \frac{0.693\ Em_2}{\tau M_o(\varepsilon_n + \varepsilon_f)}e^{-0.693\ t/\tau} \qquad (A27)$$

Substituting this expression into Eq. (A25) yields

$$a_r = \frac{0.693\ Ee^{-0.693\ t/\tau}}{M_o\tau c(1 + \mu)\left(1 + \frac{m_1 + m_3}{m_2}\right)}\left(\frac{\varepsilon_r - \varepsilon_f}{\varepsilon_r + \varepsilon_f}\right) \qquad (A28)$$

Note that this acceleration is independent of temperature if the mass ratios are independent of temperature.

Representative values of achievable emissivities are $\varepsilon_r \approx 0.9$ (attainable with oxidized metal surfaces) and $\varepsilon_f \approx 0.3$ (for several polished metals). With these values, the initial radiative accelerations become:

For Cf^{254}:

$$a_r = \frac{0.017}{(1 + \mu)\left(1 + \frac{m_1 + m_3}{m_2}\right)} m/sec^2 \qquad (A29)$$

and for Po^{210}:

$$a_r = \frac{2.36 \times 10^{-4}}{(1 + \mu)\left(1 + \frac{m_1 + m_3}{m_2}\right)} m/sec^2 \qquad (A30)$$

For comparison, solar-sail accelerations, using available thicknesses of aluminized plastic sheet ($m_s \approx 5 \times 10^{-3}$ kg/m^2) are of order 2.5×10^{-3} m/sec^2 at Earth orbit with $\mu = 0.1$. Thus, if the substrate and retention layer thicknesses can be kept comparable to the active-film thickness, the acceleration due to differential radiation can be considerably greater for Cf^{254} thrust sheet than that attainable with solar sails at Earth orbit.

Equation (A27) permits calculating the maximum allowable active-film layer thickness ($m_2 = \rho_2 d_2$) as function of tolerable sheet temperature T_m. For the fission thrust sheet using Cf^{254} (E = 200 MeV) the result is

$$m_{2,max} = 5.6 \times 10^{-15}(\varepsilon_r + \varepsilon_f)T_m^4 \ kg/m^2 \qquad (A31)$$

and for Po^{210} (E = 5.3 MeV)

$$m_{2,max} = 4.0 \times 10^{-13}(\varepsilon_r + \varepsilon_f)T_m^4 \ kg/m^2 \qquad (A32)$$

At a value of $T_m = 1000$ K, the emissivities $\varepsilon_r = 0.9$, $\varepsilon_f = 0.3$ yield:

For Cf^{254}:

$$m_{2,max} = 6.7 \times 10^{-3} \ kg/m^2 \qquad (A33)$$

and for Po^{210}:

$$m_{2,max} = 0.48 \ kg/m^2 \qquad (A34)$$

For a density of $\rho = 18 \times 10^3$ kg/m^3 which is typical of heavy elements, these values lead to active-film thicknesses of 3.7×10^{-7} m (3700 Å) for Cf^{254} and 2.7×10^{-5} m for Po^{210}. Using Eq. (A10) for r_m yields, for Cf^{254}:

$$\left(\frac{d_2}{r_m}\right)_{max} = \frac{3.7 \times 10^{-7}}{5.58 \times 10^{-6}} = 0.067 \qquad (A35)$$

and for Po^{210}:

$$\left(\frac{d_2}{r_m}\right)_{max} = \frac{2.7 \times 10^{-5}}{10^{-5}} = 2.7 \qquad (A36)$$

Thus, one concludes that for the fission-powered thrust sheet, the maximum active-film thickness may be limited by the permissible operating temperature of the sheet, while for the α-emitting thrust sheet, the temperature attained by the thrust sheet should be no problem.

Optimization of Layer Thicknesses

If no restriction exists on the thickness of the layers other than to maximize the mission capability, then for any spontaneous-emission process, one should maximize the factor $f(d_2/r_m, d_1/d_2)$ in Eq. (A22). This equation assumes, however, that only rearward emission takes place. If the substrate thickness, d_3, is less than r_m, some of the emitted particles will emerge in the forward direction, thereby reducing the net acceleration. But a reduction of d_3/d_2, in the denominator of the Eq. (A22) reduces the residual mass and thus tends to increase the net acceleration. Hence, an optimum d_3 may occur which is less than r_m. To analyze this situation, one may note that the expressions for the thrust in the $(-x)$ direction due to forward-penetrating particles are obtained by substituting d_3 for d_1 in the numerator of Eq. (A22). Thus the maximum net thrust/mass ratio due to particle ejection is obtained by maximizing the expression

$$f_{net} = f\left(\frac{d_2}{r_m}, \frac{d_1}{d_2}\right) - f\left(\frac{d_2}{r_m}, \frac{d_3}{d_2}\right) \quad (A37)$$

Ideal thrust sheet ($d_1 \ll d_2$): If it is found that the material-retention layer-thickness, d_1, can be negligibly small compared to the active-film thickness, d_2, then Eq. (A37) becomes:

$$f_{net} = \frac{\frac{d_2}{r_m}\frac{d_3}{d_2}\left(1 + 2a - 2a\frac{d_2}{r_m} - 2a\frac{d_2}{r_m}\frac{d_3}{d_2}\right)}{8\left(1 + \frac{d_3}{d_2}\right)} \quad (A38)$$

Maximizing f_{net} with respect to d_3/d_2 yields:

$$\left(\frac{d_3}{d_2}\right)_{opt} = \sqrt{\left(1 + \frac{1}{2a}\right)\frac{r_m}{d_2} - 1} \quad (A39)$$

Substituting this expression into (A38) yields:

$$f_{net} = \frac{1}{8}\left[(1 + 2a)\frac{d_2}{r_m} - 2\sqrt{2a(1 + 2a)}\left(\frac{d_2}{r_m}\right)^{3/2} + 2a\left(\frac{d_2}{r_m}\right)^2\right] \quad (A40)$$

Maximizing this expression now with respect to d_2/r_m yields

$$\left(\frac{d_2}{r_m}\right)_{opt} = \frac{1}{4}\left(1 + \frac{1}{2a}\right) \quad (A41)$$

and the maximum value of f_{net} becomes

$$f_{net,m} = \frac{a}{64}\left(1 + \frac{1}{2a}\right)^2 \quad (A42)$$

Equation (A39) becomes, for both values of a:

$$\left(\frac{d_3}{d_2}\right)_{opt} = 1 \quad (A43)$$

Using these values, together with Eqs. (A10), (A23), and (A24) yields the following optimum parameters for the two spontaneous-emission thrust sheets (for $\mu = 0.1$):

For Cf^{254}:

$$\frac{d_2}{r_m} = \frac{3}{8}; \qquad \frac{d_3}{d_2} = 1$$

$$m_3 = m_2 = \frac{3}{8}(\rho r_m) = 0.0375 \text{ kg/m}^2$$

$$d_2 = \frac{m_2}{18\times10^3} = 2.1\times10^{-6} \text{ m} \qquad \Big\} \quad (A44)$$

$$f_{net} = 0.035$$

$$a_o = 0.025 \text{ m/sec}^2$$

For Po^{210}:

$$\frac{d_2}{r_m} = \frac{1}{2}, \qquad \frac{d_3}{d_2} = 1$$

$$m_3 = m_2 = \frac{1}{2}(\rho r_m) = 0.091 \text{ kg/m}^2$$

$$d_2 = 5.1\times10^{-6} \text{ m} \qquad \Big\} \quad (A45)$$

$$f_{net} = 0.031$$

$$a_o = 5\times10^{-4} \text{ m/sec}^2$$

It is interesting to compare these optimized thrust/mass ratios due to particle emission with the values attainable by differential thermal radiation. Using the values $m_3/m_2 = d_3/d_2 = 1$, Eqs. (A29) and (A30) yield:

For Cf^{254}:

$$a_r = 7.7\times10^{-3} \text{ m/sec}^2 \quad (A46)$$

For Po^{210}:

$$a_r = 1.07\times10^{-4} \text{ m/sec}^2 \quad (A47)$$

These values are, respectively, 32 and 21 percent of the particle-emission thrust/mass ratio.

One might next inquire, since radiation and particle emission thrusts can be of the same order, whether it might be more advantageous to maximize the former rather than the latter. To do this, Eqs. (A29) and (A30) show that it is necessary to minimize the ratio of substrate and retention film mass to the active-film mass. If this ratio can be kept much less than unity, these equations show that differential-radiation thrust/mass ratio could

8

approach the optimized particle-emission values. However, unless there are substantial fabrication or operational advantages, it appears preferable to optimize the particle-emission thrust and accept any additional radiative thrust that can be realized.

For the optimized thicknesses calculated above, the propellant mass ratios (Eq. (A6)), effective exhaust velocities (Eqs. (A17) and (A19)) and resulting velocity increments (Eq. (1)), are as follows:

For Cf^{254}:

$$\left.\begin{array}{c} \dfrac{m_p}{m_o} = 0.11 \\[2ex] v_j = 0.157\, v_m = 1.9 \times 10^6 \text{ m/sec} \\[2ex] \Delta v = 0.018\, v_m = 2.16 \times 10^5 \text{ m/sec} \\[2ex] m_s = m_2 + m_3 = 0.075 \text{ kg/m}^2 \end{array}\right\} \quad (A48)$$

For Po^{210}:

$$\left.\begin{array}{c} \dfrac{m_p}{m_o} = 0.0034 \\[2ex] v_j = 0.188\, v_m = 3.0 \times 10^6 \text{ m/sec} \\[2ex] \Delta v = 6.4 \times 10^{-4}\, v_m = 1.02 \times 10^4 \text{ m/sec} \\[2ex] m_s = m_2 + m_3 = 0.18 \text{ kg/m}^2 \end{array}\right\} \quad (A49)$$

(For comparison of mass densities, the value for household aluminum foil is about 0.03 kg/m².)

If the thermal-emission accelerations are added to the particle-emission values, the total initial accelerations are:

For Cf^{254}:

$$\left.\begin{array}{l} a_o = 0.033 \text{ m/sec}^2 \\[2ex] \text{For } Po^{210}: \\[2ex] a_o = 6.1 \times 10^{-4} \text{ m/sec}^2 \end{array}\right\} \quad (A50)$$

The parameters in Eqs. (A44) through (A50) are assumed to be the characteristic values for mission calculations and for comparison with other propulsion concepts in Figs. 1 and 2.

Equation (A31) shows that the optimum value $m_2 = 0.0375$ kg/m² for Cf^{254} yields a thrust-sheet temperature of 1537 K, which is probably tolerable for some metallic films (refractory metals) from the standpoint of vaporization rate. If, however, a temperature limit of 1000 K is imposed (i.e., $d_2/r_m = 0.067$ (Eq. (A35)) the derivation of optimum parameters starting with Eq. (A39) yields:

$$\left.\begin{array}{c} \left(\dfrac{d_3}{d_2}\right)_{opt} = 3.73; \qquad m_2 = 6.7 \times 10^{-3} \text{ kg/m}^2 \\[2ex] f_{net} = 0.015 \\[2ex] \dfrac{m_p}{m_o} = 0.011; \qquad v_j = 2.8 \times 10^6 \text{ m/sec} \\[2ex] \Delta v = 3.1 \times 10^4 \text{ m/sec} \\[2ex] m_s = m_2 + m_3 = 0.03 \text{ kg/m}^2 \\[2ex] a_{o,p} = 0.011 \text{ m/sec}^2; \qquad a_r = 0.0034 \text{ m/sec}^2 \end{array}\right\} (A51)$$

where $a_{o,p}$ is particle-emission acceleration and a_r is thermal-emission radiation. Thus, the total thrust/mass ratio ($a_o = 0.014$ m/sec²) is reduced to about half of the maximum value for optimized film thicknesses, if a temperature limit of 1000 K is imposed.

Stresses in Thrust Sheet

Since the fission-powered thrust sheet is subject to intense radiation damage from fission fragments, it is of interest to estimate the stress that the sheet must tolerate. The pressure, p, on the sheet is $p = m_o a$, and since $a = 0.025$ m/sec², $m_o = 0.04$ kg/m², this pressure is of order 10^{-3} N/m². If the sheet is circular, of radius r, and if the substrate (of thickness d_3) is the primary support, the stress in that substrate is obtained from

$$\sigma_3 = \frac{pr}{2d_3} = 10^{-3}\, \frac{r}{2d_3} \qquad (A52)$$

If $d_3 = d_2 = 2 \times 10^{-6}$ m, then

$$\sigma_3 = 250\, r \text{ N/m}^2 \qquad (A53)$$

For a sheet of radius 10^2 m (which would provide a total thrust of 30 Newtons, and accelerate a total mass of 1200 kg) the stress is only 2.5×10^4 N/m² (≈ 4 psi). Thus, it appears that even a badly radiation-damaged thrust sheet should be capable of withstanding the stresses associated with thrust.

Effects of Active-Film and Substrate Thickness

As indicated by Eq. (A33) an active-film thickness of 6.7×10^{-3} kg/m² produces a sheet temperature of 1000 K using Cf^{254}. An optimum substrate thickness is 3.7 times this value (Eq. (A51)), yielding a total mass thickness of 0.031 kg/m². If it is desired to reduce the operating temperature, the active-film and substrate thicknesses must be reduced proportionately. To achieve a temperature of 400 K, which would permit use of a plastic substrate[22] such as that contemplated for solar sails and laser-propelled sheets, Eq. (A31) shows that m_2 must be reduced to 1.7×10^{-4} kg/m², and the substrate to 6×10^{-4} kg/m²; which is almost an order of magnitude lower than the thickness now available. If the substrate thickness is increased to an available value ($\approx 5 \times 10^{-3}$ kg/m²), the residual mass increases rapidly, and the acceleration decreases. Hence, a plastic substrate appears to be unusable. Instead, a metallic foil, capable of

temperature above 1000 K seems to be required. Such a foil could presumably also act as the retention film for the forward surface of the active film.

If the rearward-surface retention film thickness, d_1, is not negligible relative to d_2, a reduction in performance results. If the ratio d_3/d_2 is maintained at the optimum value of 1.0 and the ratio d_2/r_m is 3/8, the expression for f_{net} (Eq. (A37)) becomes:

$$f_{net} = \frac{0.027 - 0.012 \dfrac{d_1}{d_2}}{2 + \dfrac{d_1}{d_2}} \qquad (A54)$$

Thus, if $d_1 = d_2$, f_{ret} is reduced from 0.0135 to 5×10^{-3}, a 60 percent reduction in acceleration. The rearward-surface retention film thickness should therefore be substantially less than the active-film thickness to avoid excessive performance loss. A value of $d_1/d_2 = 0.1$ yields only a 4 percent reduction in f_{net} and permits a retention film thickness of about 200 nm (2000 Å) for the optimized Cf^{254} thrust sheet. This may be adequate, according to data given in Rev. 20, wherein either carbon or gold cover films of thickness 3×10^{-4} kg/m^2 were found to prevent escape of Cf^{252} for a one-hour test time. This thickness is less than 1 percent of the optimized Cf^{254} film thickness (Eq. (A44)).

Appendix B

Comparison Mission for Solar Sail Propelled Vehicle

For comparison with the field-free trajectories used for the other propulsion concepts in Fig. 2, an appropriate mission for a solar-sail propelled vehicle might be one which moves rapidly away from the sun, starting at Earth's orbit, and neglecting the sun's gravitation field. Although this approximation is not very good for solar sails (or for the Po^{210} thrust sheet) because of the low acceleration relative to the gravitational acceleration of the sun, it is nevertheless used to provide an order of magnitude comparison.

With this assumption, the radial acceleration for a solar-sail propelled vehicle with sail normal to the Sun direction is

$$\ddot{r} = a_o \left(\frac{r_E}{r}\right)^2 = \frac{\left(\dfrac{2p_{SE}}{c}\right)\left(\dfrac{r_e}{r}\right)^2}{(1 + \mu)m_s} \qquad (B1)$$

where p_{SE} is the solar radiation power density (W/m^2) at Earth's orbit and r_E is the Earth orbit radius. Since $p_{SE} \approx 1.3 \times 10^3$ W/m^2, the initial thrust/mass ratio is:

$$a_o = \frac{8.7 \times 10^{-6}}{(1 + \mu)m_s} \qquad (B2)$$

Let $R = r/r_E$ and $T = t/t_1$ where $t_1 = (r_E/a_o)^{1/2}$. Then Eq. (B1) becomes

$$R^2 R'' = 1 \qquad (B3)$$

where $R'' = d^2R/dT^2$. (In a similar derivation for the laser-propelled thrust sheet[7] the constant of Eq. (B3) was two instead of one because the reference time, t_1, was defined differently.) First integration yields

$$R' = \sqrt{2}\,(1 - R^{-1})^{1/2} \qquad (B4)$$

which yields an asymptotic velocity ($R \to \infty$) of

$$v_{max} = \sqrt{2r_e a_o} = \frac{1613}{\sqrt{(1 + \mu)m_s}} \text{ m/sec} \qquad (B5)$$

This value can be considered to be the Δv capability of the solar sail for comparison with other systems for flyby missions.

Integration of Eq. (B4) yields the trajectory equation:

$$\sqrt{2}\,T = \sqrt{R(R - 1)} + \ln[\sqrt{R} + \sqrt{R - 1}] \qquad (B6)$$

In this equation, R is distance from the Sun in A.U. and the trip time in days is given by

$$t = 1520\sqrt{(1 + \mu)m_s}\,T \qquad (B7)$$

Results are compared with the other systems in Fig. 2 for $m_s = 5 \times 10^{-3}$ (corresponding to a thickness of 0.15 mil which, according to Ref. 22, is available in polyester film). For this thickness, Eq. (B5) yields

$$v_{max} = (\Delta v)_{eff} = 2.2 \times 10^4 \text{ m/sec} \qquad (B8)$$

and Eq. (B2) yields:

$$a_o = 1.6 \times 10^{-3} \text{ m/sec}^2 \qquad (B9)$$

These values are somewhat better than those for the Po^{210} thrust sheet, but much less than those for the Cf^{254} thrust sheet.

References

1. Moeckel, W. E., "Propulsion Systems for Manned Exploration of the Solar System," Astronautics and Aeronautics, Vol. 7, Aug. 1969, pp. 66-77.

2. Moeckel, W. E., "Comparison of Advanced Propulsion Concepts for Deep Space Exploration," Journal of Spacecraft and Rockets, Vol. 9, Dec. 1972, pp. 863-868. (Also see NASA TN D-6968, Sept. 1972.)

3. Sänger, E., "Photon Propulsion," Handbook of Astronautical Engineering, H. H. Koelle, ed., 1st ed., McGraw-Hill Book Co., New York, 1961, pp. 21-88 to 21-98.

4. Papailiou, D. D., ed., "Frontiers in Propulsion Research: Laser, Matter-Antimatter, Excited Helium, Energy Exchange Thermonuclear Fusion," Report JPL-TM-33-722, Mar. 1975, Jet Propulsion Lab., Pasadena, Calif.; also CR-142707, NASA.

5. Garwin, R. L., "Solar Sailing - A Practical Method of Propulsion Within the Solar System," Jet Propulsion, Vol. 28, Mar. 1958, pp. 188-190.

6. Tsu, T. V., "Interplanetary Travel by Solar Sail," American Rocket Society Journal,

Vol. 29, June 1959, pp. 422-427.

7. Moeckel, W. E., "Propulsion by Impinging Laser Beams," _Journal of Spacecraft and Rockets_, Vol. 9, Dec. 1972, pp. 942-944.

8. Moeckel, W. E., et al., "Satellite and Space Propulsion Systems," NASA TN D-285, 1960.

9. "Chart of the Nuclides," General Electric Co., 1972.

10. Hooshyar, M. A., and Malik, F. Barry, "Total Spontaneous Fission Half-Lives, Kinetic Energy and Mass Yield Spectra at 250 Cm, ^{254}Cf and ^{358}Fm," _Helvetica Physica Acta_, Vol. 46, 1973, pp. 724-728.

11. Khan, A. M. and Knowles, J. W., "Photofission of ^{232}Th, ^{238}U, and ^{235}U Near Threshold Using a Variable-Energy Beam of γ-Rays," _Nuclear Physics_, Vol. 179A, 1972, pp. 333-352.

12. Alm, A. and Kivikas, T., "Experimental Study of Mass Asymmetry in Subbarrier Photofission of ^{238}U," _Nuclear Physics_, Vol. 215A, 1973, pp. 461-470.

13. Kondrat'ko, M. Ya, Korinets, V. N., and Petrzhak, K. A., "Distribution of Masses of Fragments in the Region of Symmetric Photofission of ^{235}U and ^{237}Np," _Soviet Atomic Energy_ (Engl. trans.), Vol. 35, Sept. 1973, pp. 866-868.

14. Baranowski, F. P., "Development and Production of Californium," _Symposium on Californium 252_, J. J. Barker, ed., CONF-681032, American Nuclear Society, New York, 1968, pp. 201-211.

15. King, L. J., Bigelow, J. E., Collins, E. D., "Transuranium Processing Plant Semi-Annual Report for Period Ending June 30, 1975," AEC-ORNL-084.

16. Bigelow, John: Personal communication. Transuranium Processing Facility, Oak Ridge National Laboratory.

17. Seaborg, G. T., "Status Report on the Transuranium Element," _XXIVth International Congress on Pure and Applied Chemistry_, Vol. 6, Butterworth (London), 1973, pp. 1-32.

18. Seaborg, G. T., "Transuranium Elements," Yale Univ. Press, New Haven, 1974.

19. Wilets, L., "Theories of Nuclear Fission," Clarendon Press, Oxford, 1964.

20. Adair, H. L., "Fission Fragment Energy Loss and Spectrum Parameter Changes for ^{252}Cf Sources Overcoated with Carbon and Gold," _Nuclear Instruments and Methods_, Vol. 100, 1972, pp. 467-472.

21. Evans, R. D., "The Atomic Nucleus," McGraw-Hill Book Co., New York, 1955.

22. "Mylar Polyester Film, Summary of Properties," Technical Bulletin M-1J, Dupont Company.
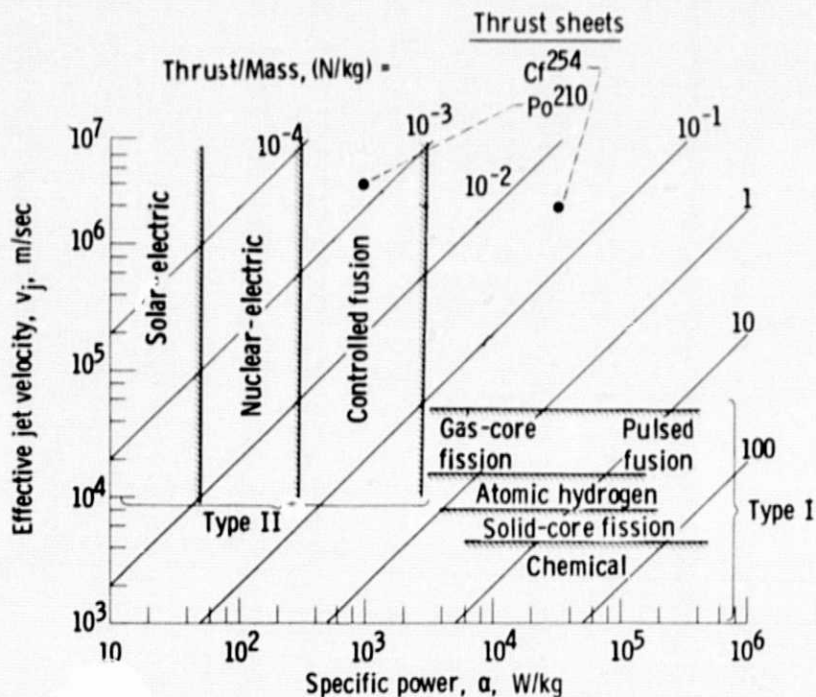
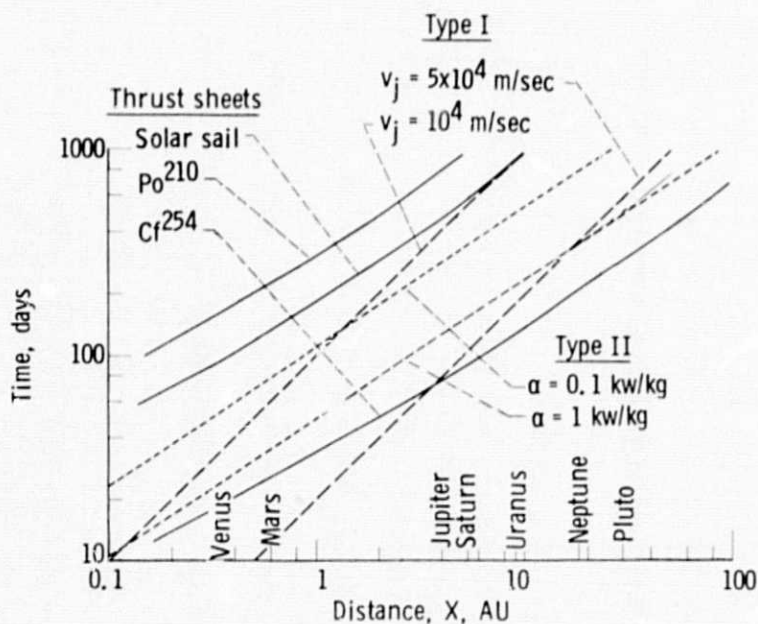Figure 1. - Propulsion system performance parameters.

Figure 2. - Flyby mission time comparison. Single stage;
payload ratio, 0.1.